Journal of Alloys and Compounds 488 (2009) 568–573

Contents lists available at ScienceDirect

Journal of Alloys and Compounds

journal homepage: www.elsevier.com/locate/jallcom

Lanthanide charge transfer energies and related luminescence, charge carrier trapping, and redox phenomena

P. Dorenbos

Delft University of Technology, Faculty of Applied Sciences, Mekelweg 15, 2629 JB Delft, The Netherlands

ARTICLE INFO

Article history:
Received 27 May 2008
Received in revised form 15 July 2008
Accepted 1 September 2008
Available online 31 October 2008

Keywords:
Phosphors
Point defects
Crystals and ligand fields
Electronic states (localized)
Luminescence

ABSTRACT

The energy of electron transfer from the valence band to a trivalent lanthanide ion provides information on the location of the ground state energy of the corresponding divalent lanthanide ion relative to the top of the valence band. It turns out that the 14 divalent lanthanides show a highly predictive pattern of the lowest 4f state energy location in compounds with the number n of electrons in the 4f shell. The lowest 4f state location controls important aspects like luminescence quantum efficiency, valence stability, and charge carrier trapping. An overview of our present state of knowledge is presented.

1. Introduction

The excitation spectrum of the red ≈ 610 nm Eu^{3+} emission in oxide compounds usually shows an intense and broad (0.6–0.8 eV) band around 250 nm. The band is due to electron transfer from an oxygen ligand to Eu^{3+}. The presence of this charge transfer (CT) excitation band makes Eu^{3+} ideally suited to sensitize the 254 nm emission of Hg in the tri-color fluorescence tube. For that reason numerous compounds with Eu^{3+} have been studied since the first use of lanthanides for lighting and display applications almost 50 years ago. Other lanthanides like Sm^{3+}, Yb^{3+}, and Tm^{3+} also show charge transfer excitation bands, yet at higher energy than for Eu^{3+}. It was realized soon that in the same compound the energy $E^{CT}(Sm)$ of CT to Sm^{3+} always appears at about 1.1 eV higher energy than $E^{CT}(Eu)$ [1–3].

In 2003 an analysis [4] on CT energies of all trivalent lanthanides in all types of compounds was performed with the aim to establish the values for the constant energy difference $\Delta E^{CT}(Ln)$ between the energy $E^{CT}(Ln)$ of CT to one specific lanthanide and $E^{CT}(Eu)$ for Eu^{3+}. In that work it was proposed that $E^{CT}(Ln)$ is a measure for the location of the ground state energy of the divalent lanthanide ion relative to the top of the valence band. Therefore the experimental value for $E^{CT}(Eu)$ in a compound together with the tabulated values for $\Delta E^{CT}(Ln)$ provide us with the location of the lowest 4f state $E_{Vf}(Ln^{2+})$ for each divalent lanthanide ion relative to the top of the valence band in that compound. In later work a tabulation of $E^{CT}(Eu)$ in about 200 different compounds was presented, and the relationship between $E^{CT}(Eu)$ and the structure and chemical properties of compounds was addressed [5].

The location of the lowest energy lanthanide $4f^n$ state relative to host lattice bands determine important properties like; luminescence quantum efficiency, charge carrier trapping phenomena, and lanthanide valence stability. An intimate relationship exists between charge transfer energies, 4f electron binding energies, ionization potentials of the free lanthanide ions, and thermodynamic properties of the pure lanthanide metals. By combining information from those different fields of rare earth science, better estimates for the parameter values needed to predict the ground state energy locations for the divalent and the trivalent lanthanides in compounds can be obtained. In this work we will review the relationship between charge transfer energies, charge carrier trapping, valence stability, free ion ionization values and properties of lanthanide metals. We will present refined values for the parameters needed to construct energy level diagrams for lanthanide in compounds.

2. Experimental data on CT energies

The energy of the CT band can be extracted from published excitation spectra of trivalent lanthanide luminescence. Fig. 1 shows data for $E^{CT}(Eu)$, $E^{CT}(Yb)$, and $E^{CT}(Sm)$ all in the same compound against $E^{CT}(Eu)$ in that same compound. The data for Eu^{3+} then fall on a line with unit slope. The data for Yb^{3+} and Sm^{3+} show a constant

E-mail address: p.dorenbos@tudelft.nl.

0925-8388/$ – see front matter © 2008 Elsevier B.V. All rights reserved.
doi:10.1016/j.jallcom.2008.09.059

Table 1
Average energy differences ΔE^{CT} between CT to Ln^{3+} and CT to Eu^{3+}. The number between brackets in column 3 and column 5 is the number of compounds used in averaging. n is the number of electrons in the $4f^n$ configuration of Ln^{3+}. $\Delta E_{Vf}(Ln^{2+})$ is the proposed energy difference between the lowest Eu^{2+} 4f state and that of another Ln^{2+}. The 'old values' are from Ref. [4] and the new ones from this work. $\Delta E_{Vf}(Ln^{3+})$ are the energy differences between the Ce^{3+} ground state and that of another Ln^{3+}. All energies are in eV.

Ln^{3+}	n	ΔE^{CT} (old)	$\Delta E_{Vf}(Ln^{2+})$ (old)	ΔE^{CT} (new)	$\Delta E_{Vf}(Ln^{2+})$ (new)	$\Delta E_{Vf}(Ln^{3+})$ (new)
La	0	–	5.19	–	5.69	–
Ce	1	–	3.87	–	4.07	0
Pr	2	2.44 (1)	2.65	2.72 (1)	2.83	−1.94
Nd	3	2.29 (1)	2.27	2.2 (1)	2.50	−3.29
Pm	4	–	2.24	–	2.32	−3.63
Sm	5	1.16 (29)	1.21	1.13 (38)	1.24	−3.74
Eu	6	0	0	0	0	−4.92
Gd	7	–	4.32	–	4.67	−6.17
Tb	8	–	3.12	–	3.23	−0.88
Dy	9	2.04 (4)	2.28	2.06 (6)	2.30	−2.53
Ho	10	2.42 (1)	2.23	2.42 (1)	2.44	−3.55
Er	11	2.26 (3)	2.43	2.34 (7)	2.62	−3.41
Tm	12	1.67 (8)	1.67	1.77 (11)	1.77	−3.18
Yb	13	0.44 (20)	0.47	0.47 (32)	0.49	−4.15
Lu	14	–	–	–	–	−5.64

energy difference with that for Eu^{3+}. Some data points may deviate considerable, but one has to realize that, for example, Sm^{3+} data stem often from an entirely different source than Eu^{3+} data. Samples do not contain the same lanthanide concentration and often are also prepared differently which may affect the energy of CT. In column 3 of Table 1 the average values for ΔE^{CT}(Ln), as were presented in Table 4 of Ref. [4], are reproduced. The numbers between brackets are the number of compounds involved in the averaging. Since 2003 new data became available and in column 5 we present revised values for ΔE^{CT}(Ln).

The old values and the new values from Table 1 are displayed in Fig. 2. Data on $Pm^{3+}$are not available because of its radioactivity, and data on La^{3+}, Ce^{3+}, Gd^{3+}, and $Tb^{3+}$are not available because the energies of CT are at too high energy. Besides for La^{2+}, Ce^{2+} and Gd^{2+} the first 5d state is at lower energy than the lowest 4f state.

Actually E^{CT}(Ln) is the energy required to remove an electron from an anion ligand minus the energy released when placing it in the 4f orbital of Ln^{3+} to create the ground state of Ln^{2+} in the host lattice. Therefore the CT energies as function of the number of electrons in 4f reflect the binding energy of the added electron in the 4f orbital. For example, the binding is strong for the half filled 4f orbital of Eu^{2+} and the completely filled 4f orbital of Yb^{2+} leading to low values for CT. The observation that the systematic variation is independent on the type of compound is linked with the shielded nature of the 4f orbital. The crystal field has then minor effect on that systematic.

Although the systematic in CT energies is almost independent on the type of compound, the absolute value E^{CT}(Ln) depends strongly on it. Fig. 3 compiles data available on E^{CT}(Eu) in about 300 different compounds. Data are grouped depending on the type of anions in the compound. The main variation with anion type is directly related with the binding strength of electrons in the anions and it can in first approximation be described by Jörgensen's empirical formula [6]

$$E^{CT} = 3.72(\chi_{opt}(x) - \chi_{opt}(m))\,\text{eV} \quad (1)$$

where $\chi_{opt}(x)$ is the optical electronegativity of the anion x from where the electron is transferred and $\chi_{opt}(m)$ is the optical electronegativity of the metal m where the electron is transferred to. $\chi_{opt}(x)$ is the same as the Pauling electronegativity, and the corrected values by Allred can be used [7]. $\chi_{opt}(m)$ is a value that must be determined empirically from observed CT energies.

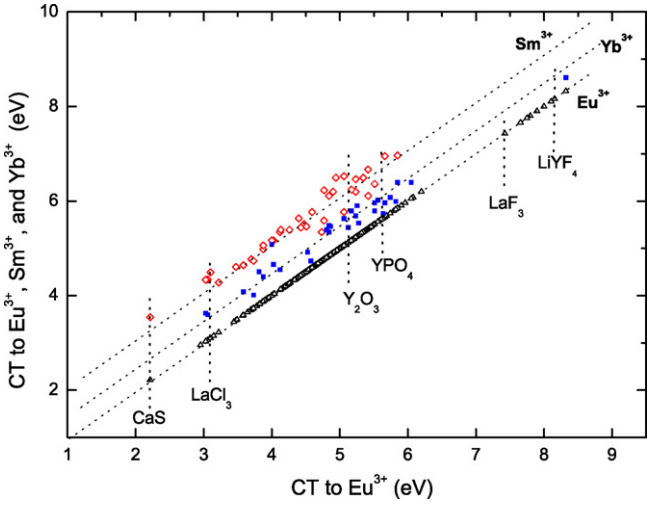

Fig. 1. Energy of charge transfer to Eu^{3+}, Yb^{3+}, and Sm^{3+}against the energy of charge transfer to Eu^{3+}in compounds. Each Eu^{3+} data point represents a different compound. The location of CT-data for various compounds is indicated by the vertical lines.

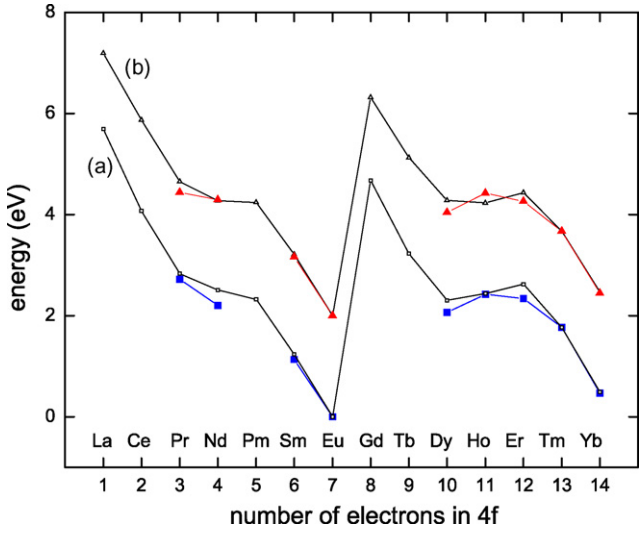

Fig. 2. The average difference in CT to Ln^{3+} with that to Eu^{3+} in compounds. Solid squares are the revised values from this work, and solid triangles are the old values from Ref. [4](displaced by +2 eV for illustration purposes). The solid curves connect the proposed values in this work (curve a) in and the old values from Ref. [4](curve b) (displaced by +2 eV for illustration purposes).

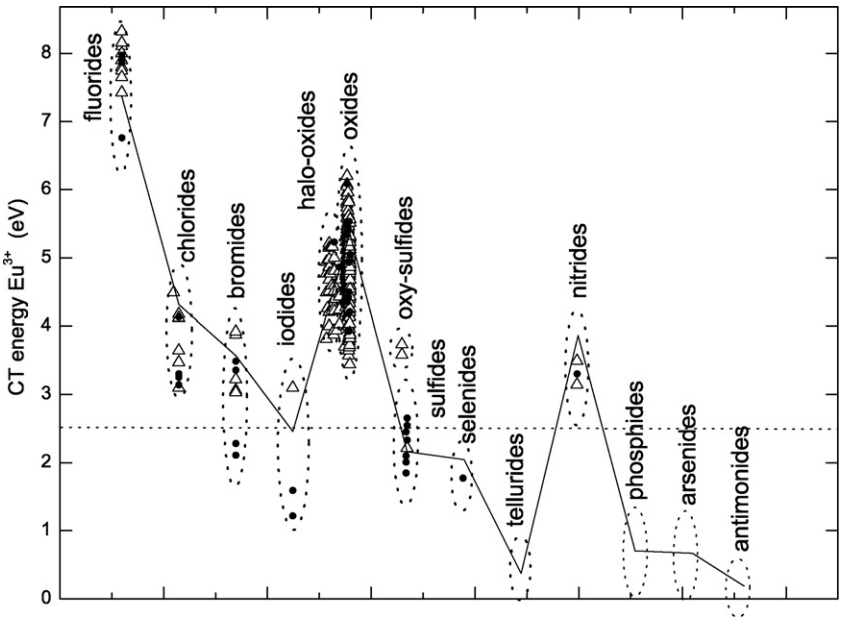

Fig. 3. The available data on energy of charge transfer to Eu^{3+}in halide, chalcogenide, and pnictide compounds. The curve through the data is obtained from Jörgensen's optical electronegativity model. Solid symbols are Eu^{3+} CT energies estimated from CT energies of lanthanides other than Eu^{3+}.

Blasse [8] argued that for CT energies smaller than the horizontal line at 2.5 eV in Fig. 3 the oxidizing power of the anions becomes too small for Eu^{3+} to be a stable valence. In those compounds Eu will adopt the divalent state spontaneously. Indeed almost all Eu^{3+} CT-data in Fig. 3 pertain to CT energies larger than 2.5 eV. However, other lanthanides like Sm^{3+} often can still be oxidized in compounds where Eu^{3+} is not stable anymore, and from CT energies to those lanthanides one may estimate $E^{CT}(Eu)$. Those estimated data are also shown in Fig. 3. Eq. (1) using $\chi_{opt}(Eu) = 2.0$ reproduces the general trend in CT energy with type of anion, but clearly a wide spread of CT values can be found within, for example, the oxide family of compounds. The binding strength of the oxygen ligands, the distance between ligands and lanthanide, the coordination number, the site size and Madelung potential, i.e., crystal structure and crystal chemistry, all affect the value for CT [5].

In excitation spectra of the red emission of Eu^{3+}in oxides the CT-band can be observed as a typically 0.6–0.8 eV wide and strong band at energies between 4 and 6 eV, see Fig. 3. After the charge transfer the transferred electron instantaneously returns to the hole left on the oxygen ligands, leaving Eu^{3+}in one of its excited $4f^6$ levels that eventually results in the intense red Eu^{3+} emission around 610 nm. There is also substantial lattice relaxation because Eu^{2+} is about 18 pm larger than Eu^{3+}. In other words there is a large Frank–Condon offset in the configuration coordinate diagram which causes that the CT bands are relatively broad. It also introduces a possible quenching route for Eu^{3+} luminescence. It was demonstrated by Struck and Fonger that the excited ^5D states of Eu^{3+} can be quenched by the CT-state especially when the CT state is at low energy [9]. In Fig. 4, data have been collected on the energy of CT to $Eu^{3+}$and the quenching temperature of Eu^{3+}emission. A clear more or less linear relationship can be observed. Y_2O_3:Eu^{3+} has the CT band at energy close to the 254 nm (4.9 eV) emission of mercury and in addition it shows high quenching temperature of Eu^{3+} emission. This phosphor is widely applied in the tri-color fluorescence tube. Recently, we proposed that the quenching of Eu^{3+} emission in $Al_xGa_{1-x}N$ near or below room temperature is also related with the small value for the CT energy [10]. Fig. 4 shows that the quenching temperature and the CT energy scale with the composition parameter x. It agrees with the observed linear relationship between CT energy and quenching temperature.

3. Charge transfer energies and absolute lanthanide level location

Since the final state in the charge transfer to Eu^{3+} is the ground state of Eu^{2+}, $E^{CT}(Eu)$ should indicate the energy E_{Vf} of the Eu^{2+} $4f^7$ ground state relative to the valence band. This idea was previously suggested by Wong et al. [11] and later used by Happek et al. [12,13] In Ref. [4] an elaborate study of such relationship was made and the assumption that the energy E^{CT} can be used for the energy E_{Vf} of the lowest 4f state above the top of the valence band was further motivated. In that work also estimates for the CT energy difference with the 'missing lanthanides' La^{3+}, Ce^{3+}, Pm^{3+}, Gd^{3+}, and Tb^{3+} were

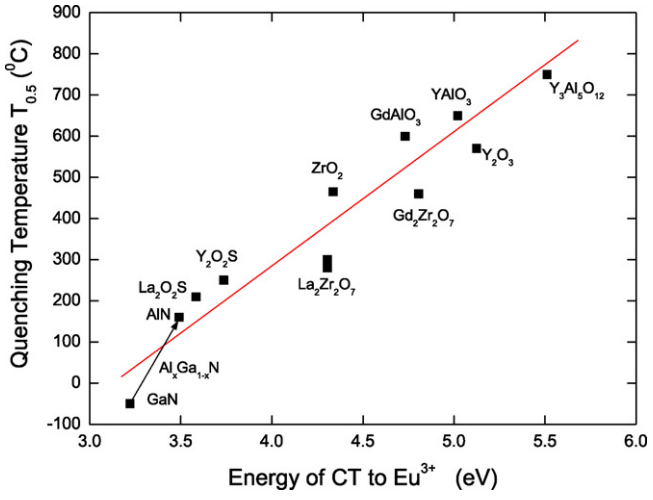

Fig. 4. The quenching temperature of Eu^{3+} emission, defined as the temperature $T^{0.5}$ at which the luminescence has dropped to 50% of the low temperature value, as function of the energy of CT to Eu^{3+}.

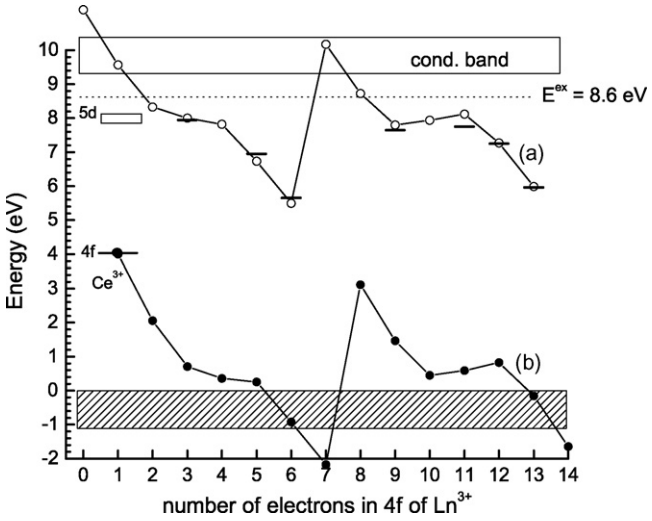

Fig. 5. The 4f ground state level location of lanthanides in YPO_4. Horizontal bars are observed energies for charge transfer to trivalent lanthanides with n electrons in 4f. Curve (a) connects the 4f ground state energies of the divalent and curve (b) of the trivalent lanthanides as function of the number n of electrons in 4f of Ln^{3+}.

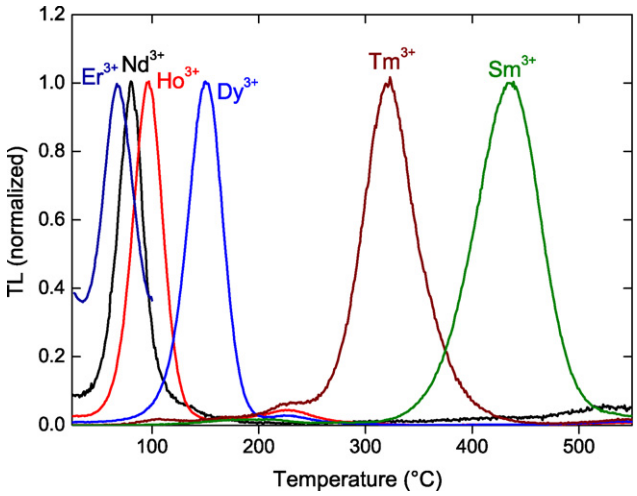

Fig. 6. Normalized thermoluminescence glow curves of YPO_4:Ce^{3+}:Ln^{3+} after β-irradiation monitoring Ce^{3+} emission (from Ref. [14]).

provided. Column 4 in Table 1 compiles the average energy difference $\Delta E^{CT}(Ln) \equiv \Delta E_{Vf}(Ln^{2+})$ between $E^{CT}(Ln)$ and $E^{CT}(Eu)$ as were proposed in Ref. [4]. The solid curve (b) in Fig. 2 connects the same data values graphically. Since publication of Ref. [4] new data on CT energies to Ln^{3+} ions became available, and also further studies were made. The revised values for $\Delta E_{Vf}(Ln^{2+})$ are compiled in column 6 of Table 1. Curve (a) in Fig. 2 connects those data graphically. Most noteworthy differences with the 'old' values are the larger values for La, Ce, Gd, and Tb and the smaller value for Dy. Details on those studies and how the revised values were obtained will be published elsewhere.

Identifying $E^{CT}(Ln)$ with $E_{Vf}(Ln^{2+})$ is an assumption that can be disputed. In an attempt to experimentally verify our assumption we decided to perform thermo-luminescence (TL) studies on YPO_4 doped with Ce^{3+} and co-doped with a second trivalent lanthanide. YPO_4 was selected because it contains only one crystallographic yttrium site that the trivalent lanthanide ion may occupy. Furthermore values for $E^{CT}(Ln)$ are well documented for YPO_4. Fig. 5 shows the level scheme constructed for YPO_4. The energy of the top of the valence band is set at zero. The horizontal bars for n = 3, 5, 6, 9, 11, 12, 13 represent $E^{CT}(Ln)$ values observed for Nd^{3+}, Sm^{3+}, Eu^{3+}, Dy^{3+}, Er^{3+}, Tm^{3+}, and Yb^{3+}. Within our model they also mark the energies of the lowest energy 4f state of the respective divalent lanthanides. The double seated curve through the data is the same as curve (a) in Fig. 2 but displaced to run best through the CT data bars. At 8.6 eV the excitation of the PO_4^{3-} group takes place and this marks the energy of the first exciton band. The bottom of the conduction band or mobility edge is estimated at around 9.3 eV [5]. The difference is the estimated electron and hole binding energy of the exciton. In the same scheme the estimated location of the ground state energy of $Ce^{3+}$is shown together with the location of its first 5d state [4].

One should not interpret the energy levels as single electron states but as total energy states. For example, the location of the ground state 4f level of Ce^{3+} at 4 eV above the top of the valence band means that it requires 4 eV less energy to remove an electron from the 4f shell of Ce^{3+} than from the top of the valence band. It also means that a hole in the valence band will be trapped by Ce^{3+} with 4 eV binding energy. Or that Ce^{4+} is 4 eV more stable than a free hole at the top of the valence band. When Sm^{3+} is doped in YPO_4 this means that the Sm^{2+} ground state is not occupied with an electron. Its location at 2.6 eV below the bottom of the conduction band implies that when Sm^{3+} traps an electron from the conduction band it will be trapped with 2.6 eV binding energy. Eu^{3+} and Yb^{3+} provide even deeper electron traps.

Recently, we performed thermo-luminescence (TL) studies on YPO_4 with Ce^{3+} and co-doped with either Pr^{3+}, Nd^{3+}, Sm^{3+}, Dy^{3+}, Ho^{3+}, Er^{3+}, or Tm^{3+}[14]. Under β-irradiation holes are created in the valence band and electrons in the conduction band. We anticipated that Ce^{3+}will be the dominant hole trap and that the other trivalent lanthanides form electron traps. The scheme of Fig. 5 predicts that the deepest one is by Sm^{3+}, followed by Tm^{3+}, Dy^{3+}, Ho^{3+}, Nd^{3+}, Er^{3+}, and finally Pr^{3+}. Fig. 6 shows the thermo-luminescence glow curves recorded after β-irradiation with an optical filter placed on the Ce^{3+} 5d–4f emission. The sequence in the temperature for the maximum of the glow peaks follows very nicely the predicted sequence from Fig. 5. The glow curve for Pr^{3+}as a co-dopant could not be measured because it occurs below room temperature which was not accessible to our TL-reader. The glow curves for $Eu^{3+}$and Yb^{3+} are expected at very high temperature also outside reach of our TL-reader.

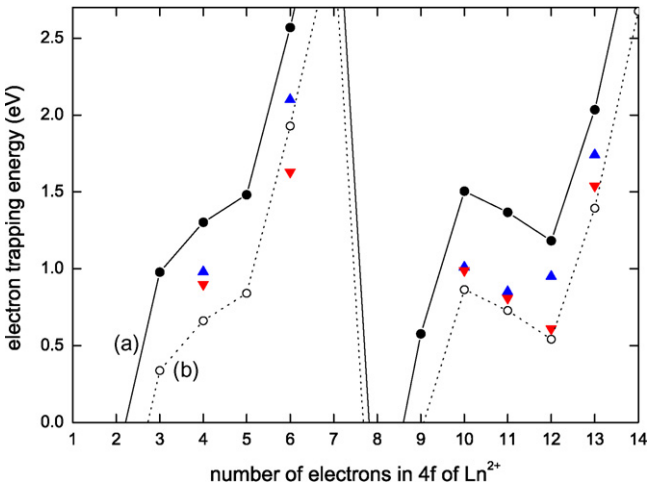

Fig. 7. Curve (a) shows the anticipated electron trapping depths provided by trivalent lanthanides in YPO_4assuming that the bottom of the conduction band is at 9.3 eV. Curve (b) the depth of electron trapping relative to the exciton state at 8.6 eV. ▽, trapping depths derived from glow curve analysis. △, trapping depths derived from the varying heating rate method (see Ref. [14] for further details).

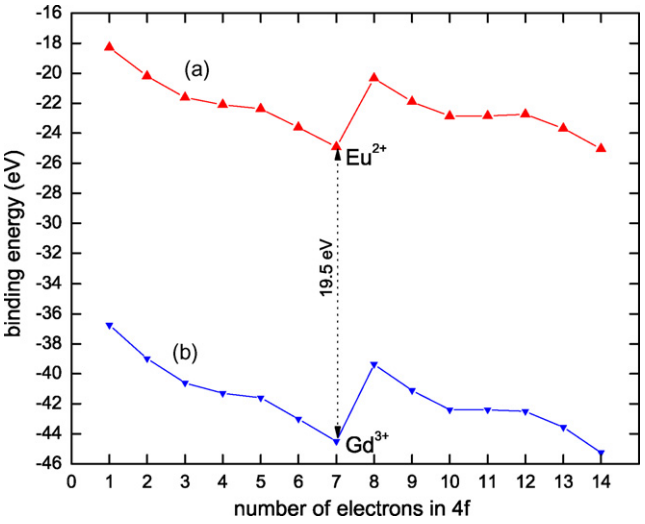

Fig. 8. The ionization energies of the free divalent and the free trivalent lanthanides from Johansson in Ref. [18].

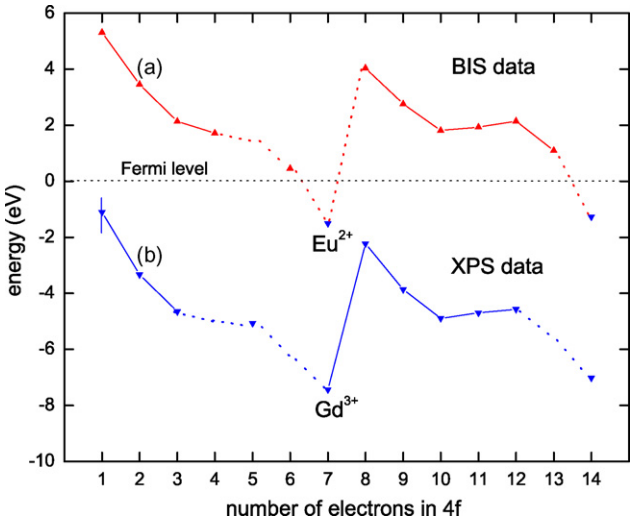

Fig. 9. The location of the 4f ground states of curve (a) divalent and curve (b) trivalent lanthanides in the pure lanthanide metals relative to the Fermi energy as obtained from XPS and BIS data. Reproduced from Ref. [20].

Fig. 7 shows results from glow curve analysis performed in Ref. [14]. Electron trapping depths derived from two different analysis methods are shown together with the trapping depths predicted from Fig. 5 as illustrated by curve (a). On average, the trapping depths from TL analysis is about 0.5 eV smaller than those predicted from Fig. 5. Actually, considering possible errors in TL analysis and a possible error in the location of the bottom of the conduction band, we regard this as a very good agreement. It is also not excluded that recombination of a trapped electron with the hole on Ce^{4+} may proceed via tail states below the bottom of the conduction band. For comparison we have also drawn (curve b) the trapping depths relative to the exciton energy of 8.6 eV. The initial assumption that the energy of charge transfer from an anion to a trivalent lanthanide provides direct information on the absolute location of the 4f ground state above the top of the valence band is therefore nicely confirmed by the TL results of Ref. [14].

4. Lanthanide-doped systems, the free lanthanide ions, and pure lanthanide metals

The previous two sections dealt with $E^{CT}(Ln)$ in inorganic compounds. It was mentioned that the variation in the energy for CT with the number of electrons in the 4f orbital relates to the variation in the binding energy of 4f electrons. These results and findings emerged from luminescence spectroscopy studies of lanthanide impurities in compounds. There are two other areas of rare earth science that provide complementary information that appears of much relevance to the lanthanide doped systems. These are the ionization energies of the free divalent and the free trivalent lanthanide ions and the properties of pure lanthanide metals.

For most of the free lanthanide ions the values for their second and third ionization potentials were not determined experimentally but are estimations that are based on experimentally known 4f–5d and 4f–6s transition energies. Fig. 8 shows the binding energies, i.e. ionization potentials, of the 4f electron in the free lanthanide ions based on such work [15–17]. The shape of curve (a) for the divalent lanthanide ions is very similar to the $\Delta E^{CT} \equiv \Delta E_{Vf}(Ln^{2+})$ curve in Fig. 2 curve (a). There are however slight but important differences. The 4f electron binding energy in the free ion Yb^{2+} is few tenths of an eV larger than that in the free ion Eu^{2+}. However, curve (a) in Fig. 2 shows that the Yb^{2+} 4f ground state energy in inorganic compounds is at about 0.5 eV higher energy than that of Eu^{2+} which implies 0.5 eV less binding energy.

Another topic that has attracted considerable attention is the chemistry and physics of the pure lanthanide metals. From XPS (X-ray photoelectron spectroscopy) and BIS (Bremsstrahlung isochromat spectroscopy) the location of the 4f levels in pure lanthanide metals is known. Fig. 9 shows those locations for the 4f states of divalent and trivalent lanthanides [20]. Apart from Eu and Yb all the lanthanide metals have the trivalent electron configuration. The three $5d6s^2$ electrons form the conduction band. We observe the same patterns as for the ionization energies of the free ions and for the ΔE^{CT} energies in lanthanide doped compounds. Note that the Yb^{2+} ground state is located at few tenths of eV above the Eu^{2+} ground state in the pure lanthanide metals. This resembles what we have observed for the $\Delta E^{CT}(Yb)$ value.

Johansson determined the energy differences $\Delta E_{II,III}$ between the heat of formation of hypothetical divalent metals with that of trivalent metals. These values were then used as a basis to estimate the $\Delta E_{III,IV}$ between trivalent metals and hypothetical four valence metals also. These ΔE values are practicaly the same as the energy differences between 4f states and the Fermi level in metals [18]. Fig. 10 compiles the two sets of ΔE values and indeed it is almost similar as in Fig. 9. The heat of formation of the lanthanide metals is know with reasonable accuracy and we regard the double seated curves in Fig. 10 as more accurate then the ones based on XPS and BIS data in Fig. 9.

Based on the $\Delta E_{III,IV}$ values Johansson [18] made also better estimates for the fourth ionization potentials of the lanthanides. Those estimated values are shown in Fig. 8. N.B. later also Thiel et al. [19] provide estimates for the fourth ionization energy of the lanthanides that agree well with those of Johansson.

Comparing the so-called double-seated curves for the free lanthanide ions in Fig. 8 with that for the pure lanthanide metals in Fig. 10 there is much similarity but also important differences. Most striking is the energy difference between the 4f ground state of the divalent with that of the trivalent lanthanides. It is about 20 eV for free ions but about 7 eV for the pure lanthanide metal. This reduction by a factor of three is attributed to an almost perfect screening of the lanthanide ion by the conduction band electrons [21]. In addition the double seated curves for the metals are tilted with respect to those for the free ions. With increase of the number of electrons

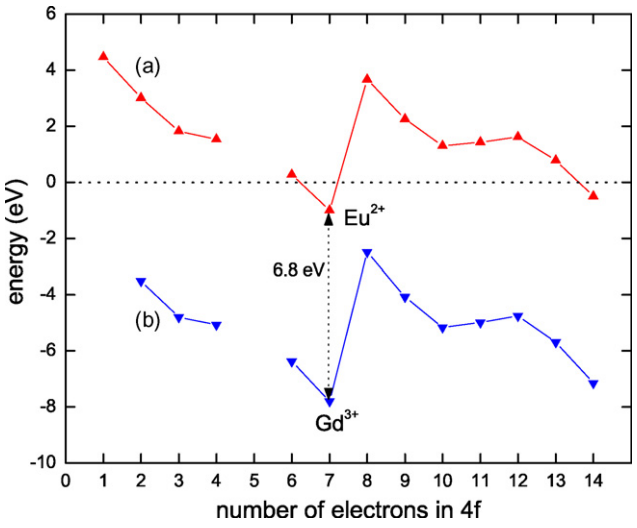

Fig. 10. The location of the 4f ground state of curve (a) divalent and curve (b) trivalent lanthanides in the pure lanthanide metals as determined from the heat of formation by Johansson in Ref. [18].

in 4f the 4f ground state energy is lifted slightly further. For example, the ground state energy of free $Yb^{2+}$is at few tenths of an eV lower energy than that of free Eu^{2+}but for the metals it is at about 0.5 eV higher energy. This is precisely the same as the value for ΔE^{CT} for Yb^{3+}, see Fig. 2 and Table 1.

The following equation has been proposed to relate the ground state 4f energy E_{4f} of lanthanides in compounds with the ionization energy I_f of the free lanthanide ions [22,19]

$$E_{4f} = I_f - E_L + \alpha_R(R - R_0) \quad (2)$$

where E_L is a constant energy shift closely related with the Madelung potential pertaining to all lanthanides similarly. The last term in Eq. (2) is a correction due to the lanthanide contraction leading to additional lattice relaxation and changing Madelung potential. In fact E_L creates a vertical energy shift of the free ion curves in Fig. 8 and the last term creates a tilting of the free ion curves, i.e., the double seated curve is lifted further with increase of n.

It turns out that with Eq. (2) the free ionization curves in Fig. 8 can be mapped almost perfectly onto the pure lanthanide metal curves of Fig. 10. By combining now the ΔE^{CT} data with the free ion ionization data and the pure lanthanide metal data, a set of values can be established that provide us with the most appropriate double seated curves for the divalent lanthanides and for the trivalent ones in compounds. By requiring self-consistency one may also refine the estimates for the third and fourth ionization potentials. Details on obtaining those refined estimates will be published elsewhere. In this work we have listed the obtained values for $\Delta E_{Vf}(Ln)$ for the divalent and the trivalent lanthanides in column 6 and column 7 of Table 1, respectively.

It is most convenient to use the energy $E^{CT}(Eu)$ of CT to Eu^{3+} as an anchor point to position the double seated curve for the divalent lanthanides in a compound as has been done in Fig. 5. This is the reason that we have specified the $\Delta E_{Vf}(Ln^{2+})$ values relative to Eu^{2+}in Table 1. One also likes to place the double seated curve for the trivalent lanthanides in the same scheme, and for that a suitable anchor point needs to be used also. This is not as easily and abundantly available as for the divalent ions. Quenching of the 5d–4f emission of Ce^{3+}due to thermally activated ionization of the 5d electron may provide us with the activation energy for ionization, and from that the absolute location of the 5d state (and then also the 4f ground state) below the conduction band can be deduced. Photoconductivity studies on Ce^{3+}doped compounds occasionally can also provide the necessary information. Presently we are exploring a new technique based on thermoluminescence studies on double doped compounds. However instead of exciting with β-irradiation, photon excitation will be used. By scanning the excitation wavelength the threshold for trap filling can be determined which in turn may provide us with the location of the Ce^{3+} 4f ground state relative to the conduction band. In Table 1 the proposed $\Delta E_{Vf}(Ln^{3+})$ values are specified relative to Ce^{3+}.

In Fig. 5 the double seated curve has been drawn based on the anchor point for the Ce^{3+} ground state at 4 eV above the valence band [4]. Note that the energy difference between the ground state of $Eu^{2+}$and the ground state of $Eu^{3+}$is 6.4 eV which is much smaller than for the free Eu ions (18 eV) but larger than for the pure Eu-metal (5.4 eV). Apparently the screening effects in ionic crystals are close to, but somewhat smaller than, in the pure lanthanide metals. We have strong indications that the energy difference between the Eu^{2+} and Eu^{3+} ground states in compounds varies from above 7 eV in poorly polarizable compounds like the fluorides to below 6 eV in strongly polarizable compounds like bromides and sulfides. It may well be that the energy difference between the Eu^{2+} ground state and the Eu^{3+} can be predicted well beforehand from the refractive index of the compound. Note that the free lanthanides and the pure lanthanide metals form the extreme ends on the 'polarizability scale', i.e. zero polarizability and zero screening for the free lanthanides and infinity polarizability and perfect screening for the lanthanide metals.

5. Conclusions

Spectroscopic information on charge transfer bands of trivalent lanthanides in compounds provides us with the location of the divalent lanthanide ground state above the valence band. Those locations are consistent with the depth of electron trapping by trivalent lanthanides that were derived from thermoluminescence studies on YPO_4:Ce^{3+}:Ln^{3+} double doped phosphors. A close relationship between lanthanide level location in impurity doped compounds with the free lanthanide ions and the lanthanide metals has been demonstrated. By exploiting information from free ion levels and pure lanthanide metals more accurate parameter values were derived to construct lanthanide level schemes in compounds.

References

[1] C.K. Jörgensen, Mol. Phys. 5 (1962) 271.
[2] J.C. Barnes, H. Pincott, J. Chem. Soc. (a) (1966) 842.
[3] G. Blasse, A. Bril, Phys. Lett. 23 (1966) 440.
[4] P. Dorenbos, J. Phys.: Condens. Matter 15 (2003) 8417.
[5] P. Dorenbos, J. Lumin. 111 (2005) 89.
[6] C.K. Jörgensen, Modern Aspects of Ligand Field Theory, North-Holland Publishing Company, Amsterdam, 1971.
[7] A.L. Allred, J. Inorg. Nucl. Chem. 17 (1961) 215.
[8] G. Blasse, N. Sabbatini, Mater. Chem. Phys. 16 (1987) 237.
[9] C.W. Struck, W.H. Fonger, J. Lumin. 1 (2) (1970) 456.
[10] P. Dorenbos, E. van der Kolk, Opt. Mater. 30 (2008) 1052.
[11] W.C. Wong, D.S. McClure, S.A. Basun, M.R. Kokta, Phys. Rev. B 51 (1995) 5682.
[12] U. Happek, S.A. Basun, J. Choi, J.K. Krebs, M. Raukas, J. Alloys Compd. 303 (2000) 198.
[13] U. Happek, J. Choi, A.M. Srivastava, J. Lumin. 94–95 (2001) 7.
[14] A.J.J. Bos, P. Dorenbos, A. Bessiere, B. Viana, Radiat. Measure. 43 (2008) 222.
[15] J. Sugar, J. Reader, J. Chem. Phys. 59 (1973) 2083.
[16] L.R. Morss, Chem. Rev. 76 (1976) 829.
[17] L. Brewer, in: S.P. Sinha, D. Reidel (Eds.), Systematics and the Properties of the Lanthanides, Publishing Company, Dordrecht, The Netherlands, 1983, p. 17.
[18] B. Johansson, Phys. Rev. B20 (1979) 1315.
[19] C.W. Thiel, Y. Sun, R.L. Cone, J. Modern Opt. 49 (2002) 2399.
[20] J.K. Lang, Y. Baer, P.A. Cox, J. Phys. F: Metal Phys. 11 (1981) 121.
[21] J.F. Herbst, D.N. Lowy, R.E. Watson, Phys. Rev. B 6 (1972) 1913.
[22] C. Pedrini, D.S. McClure, C.H. Anderson, J. Chem. Phys. 70 (1979) 4959.